**Proceedings of ASME 2016 Dynamic Systems and Control Conference**
**DSCC 2016**
**October 12-14, 2016, Minneapolis, Minnesota, USA**

**DSCC2016-9858**

# DRAFT: DAMAGE DETECTION OF BRIDGE NETWORK WITH SPATIOTEMPORAL PATTERN NETWORK

Chao Liu[1], Yongqiang Gong[2], Simon Laflamme[2], Brent Phares[2], Soumik Sarkar[1]
{cliu5,laflamme,bphares,soumiks}@iastate.edu
[1]Department of Mechanical Engineering, [2]Department of Civil, Construction and Environmental Engineering
Iowa State University, Ames, IA 50011, USA

## ABSTRACT

*The alarmingly degrading state of transportation infrastructures combined with their key societal and economic importance calls for automatic condition assessment methods to facilitate smart management of maintenance and repairs. In particular, scalable data-driven approaches is of great interest, because it can deal with large volume of streaming data without requiring models that can be inaccurate and computationally expensive to run. Properly designed, a data-driven methodology could enable fast and automatic evaluation of infrastructures, discovery of causal dependencies among various sub-system dynamic responses, and inference and decision making with uncertainties and lack of labeled data. In this work, a spatiotemporal pattern network (STPN) strategy built on symbolic dynamic filtering (SDF) is applied to explore spatiotemporal behaviors in bridge network. Data from strain gauges installed on two bridges are simulated by finite element method, and the causality among strain data in spatial and temporal resolutions is analyzed. Case studies are conducted for truck identification and damage detection from simulation data. Results show significant capabilities of the proposed approach in: (i) capturing spatiotemporal features to discover causality between bridges (geographically close), (ii) robustness to noise in data for feature extraction, and (iii) detecting and localizing damage via the comparison of behaviors within the bridge network.*

## 1 INTRODUCTION

The number of civil structures with critical aging concerns is large; the cost of repairing and upgrading them is estimated at $2.2 trillion [1–3]. In the United States alone, the average age of the 607,380 bridges is 42 years, and the Federal Highway Administration (FHWA) estimated that we would need to invest $76 billion to repair deficient bridges. This and other recent infrastructure failures have raised serious concerns about the structural integrity of the aging and deteriorating civil infrastructures around the world, about the inefficiency, ineffectiveness and non-uniformity of visual inspection, which is still the prevalent method for infrastructure inspection, and about societies' readiness to respond, to mitigate, to forecast, to manage, and to minimize the risks associated with aging infrastructures. A solution is to automate the condition assessment process, also known as structural health monitoring (SHM).

SHM of civil infrastructures (e.g., bridges, wind turbines, buildings, nuclear structures, etc.) is a difficult task due to the large geometries under inspection. A fundamental challenge is the lack of scalability of existing sensing solution, due to economic and/or technical challenges associated with off-the-shelf sensors. For example, resistive foil gauges are widely used to monitor existing cracks, but are geometrically too small to be capable of detecting a new damage of a large area within an acceptable level of probability [4]. A solution is to deploy sensor networks such as piezoelectric wafer active sensors networks [5, 6], fiber optics-based technologies [7, 8], embedded distributed networks of conductive particles [9, 10], and large-area electronics [4, 11, 12].

While the condition assessment research community is extremely active in developing tools and methodology enabling automatic evaluation of transportation infrastructure, the vast majority of the effort is on the input-model-output perspective,

at a single system level (e.g., a structure equipped with sensors). The problem is not typically approached in terms of systems of systems (e.g., many interacting structures on a network equipped with sensors). There has been some research conducted in the evaluation of infrastructure systems resiliency, that investigated infrastructures as an interconnected system. These studies mainly studied the impact of that a bridge closure would have on an entire network, and did not consider the integration of sensor data. See references [13–16] for instance. There is an important opportunity in agglomerating local networks of sensors for improving the condition assessment process, which constitute a system of systems, also termed complex system.

Here, we propose to leverage the unique spatial properties of bridges in a transportation network to evaluate their conditions in a complex system framework. Bridges constitute critical connection points in the transportation system. In additional, adjacent bridges in a system have typically very similar vehicle loads, weather condition, and geological condition. In the spatial and temporal space, the behavior of the bridges are relative, noted as causality in graph theory. Discovering the spatiotemporal features in the bridge system is beneficial in detecting potential changes in structural integrity, and improving the efficiency and accuracy of bridge inspections by providing the inspectors with useful data for guidance and identification of potential problems, instead of uniquely relying on visual procedures and the inspector's judgement.

The spatiotemporal discoveries will be made through the comparison of intrinsic geometry of data sets. This idea has been previously applied in the field of SHM. For instance, [17] used a multivariate attractor-based approach to detect the presence and magnitude of damage in structures through the investigation of the response's phase-space constructed by a time delayed embedding. Ref. [18] compared an attractor constructed from the undamaged state to predict structural response, and identified damage as a change in the prediction error. In [19], the dynamic system is divided in subsystems to cope with nonlinearities, and the time series response of each subsystem is analyzed. The study in [20] proposed to analyze nonlinear time series using a multivariate autoregressive approach in order to detect damage under varying operational and environmental conditions. Ref. [21] used a combined state-space embedding strategy and singular value decomposition to detect structural damage. Refs [12, 22, 23] used a diffusion map-based approach for detection of anomaly in dynamic systems.

Pattern discoveries in spatiotemporally distributed systems can also be conducted using symbolic dynamic filtering (SDF) [24] for establishing and representing causal interactions among the subsystems [25]. SDF, as a data driven dynamical system modeling technique, has advantages in describing different types of data with a uniform symbolic representation as well as low time and memory complexity. Symbolic time-series features captured by SDF can be used in formation of spatiotemporal pattern network (STPN) as reported in recent studies [26, 27].

In this work, we build on STPN to explore spatiotemporal behaviors in a network of bridges from a condition monitoring perspective. Data of strain gauges in the bridges are simulated by finite element method, and analyzed using STPN. The causality (the causes and the effects) of strain data in spatial and temporal resolutions is applied for damage detection and localization in bridges, as the causality includes critical features of the dynamical system health and has great potential in detecting damage and reasoning failure scenarios. Case studies are conducted based on strain data of two adjacent bridges simulated with various vehicle (truck) types as well as different damage levels.

## 2 Background and preliminaries

### 2.1 Spatiotemporal pattern network

SDF has been recently shown to be extremely effective for extracting key textures from time-series data [24]. The main idea is that a symbol sequence (i.e., discretized time-series) emanated from a process can be approximated as a Markov chain of order $D$ (also called depth), named as $D$-Markov machine [25] that captures the essential behavior of the underlying process.

The discretization or symbolization process is noted as partitioning [24]. Let $\mathbb{X}$ denote a set of partitioning functions, $\mathbb{X}: X(t) \to S$, that transforms a general dynamic system (time series $X(t)$) into a symbol sequence $S$ with an alphabet set $\Sigma$. Various approaches are proposed in the literature, depending on different objective functions, such as uniform partitioning (UP), maximally bijective discretization (MBD) [28], statistically similar discretization (SSD) [29], and maximum entropy partitioning (MEP). This study uses simple uniform partitioning.

The $D$-Markov machine is essentially a probabilistic finite state automaton (PFSA) that can be described by states (representing various parts of the data space) and probabilistic transitions among them that can be learnt from data. Related definitions of deterministic finite state automaton (DFSA), PFSA, $D$-Markov machine, $xD$-Markov machine and the learning schemes can be found in [25].

With this setup, a spatiotemporal pattern network (STPN) is defined below [27].

**Definition**. A PFSA based STPN is a 4-tuple $W_D \equiv (Q^a, \Sigma^b, \Pi^{ab}, \Lambda^{ab})$: (a, b denote nodes of the STPN)

(1) $Q^a = \{q_1, q_2, \cdots, q_{|Q^a|}\}$ is the state set corresponding to symbol sequences $S^a$;
(2) $\Sigma^b = \{\sigma_0, \cdots, \sigma_{|\Sigma^b|-1}\}$ is the alphabet set of symbol sequence $S^b$;
(3) $\Pi^{ab}$ is the symbol generation matrix of size $|Q^a| \times |\Sigma^b|$, the $ij^{th}$ element of $\Pi^{ab}$ denotes the probability of finding the symbol $\sigma_j$ in the symbol string $s^b$ while making a transition from the state $q_i$ in the symbol sequence $S^a$; while self-symbol generation matrices are called atomic patterns

(APs) i.e., when $a = b$, cross-symbol generation matrices are called relational patterns (RPs) i.e., when $a \neq b$.

(4) $\Lambda^{ab}$ denotes a metric that can represent the importance of the learnt pattern (or degree of causality) for $a \rightarrow b$ which is a function of $\Pi^{ab}$.

### 2.2 Information based metric for causality

With the definition of STPN, patterns discovered between the vertices can be applied to interpret the causality via proper metrics. Information based criteria are usually applied, e.g., transfer entropy [30] and mutual information [25, 31]. This work applies mutual information for representing $\Lambda^{ab}$ of the patterns (APs & RPs). Definition of mutual information for $\Lambda^{ab}$ is as follows.

$$\Lambda^{ab} \triangleq I^{ab} = I(q^b_{k+1}; q^a_{k+1}) = H(q^b_{k+1}) - H(q^b_{k+1}|q^a_k) \quad (1)$$

Detailed description of mutual information based causality metric in the context of APs and RPs can be found in [25].

### 2.3 Similarity metric for STPNs

As a kind of graphical model, STPN can adopt metric for estimating similarity of graphs. However, most of the metrics in graphs are defined with the binary values (0/1) of the vertices/edges [32], and they are not considering influence of degree of causality (represented by mutual information in this work) among the edges. To consider the degree of causality in estimating similarity between STPNs, this work applies structural similarity (SSIM). SSIM was first proposed and applied in image processing, and it was demonstrated to be more effective in image quality assessment [33] and feature extraction [34].

Considering full connections (APs & RPs) between $n$ nodes in an STPN, a matrix with causality metric $n \times n$ is formed. Treating the causality matrix as $n$ vectors in an image (similar to the definition of SSIM in image quality assessment [33]), SSIM can be applied to estimate the similarity between two causality matrices in two STPNs. The general form of the structure similarity index [33] between two vectors $x$ and $y$ is

$$S(x,y) = \left(\frac{2\mu_x\mu_y + C_1}{\mu_x^2 + \mu_y^2 + C_1}\right)^{\alpha} \left(\frac{2\sigma_x\sigma_y + C_2}{\sigma_x^2 + \sigma_y^2 + C_2}\right)^{\beta} \left(\frac{\sigma_{xy} + C_3}{\sigma_x\sigma_y + C_3}\right)^{\gamma}, \quad (2)$$

where $\mu_x$, $\mu_y$ are the means of $x$ and $y$ respectively, $\sigma_x^2$, $\sigma_y^2$ are the variances of $x$ and $y$ respectively, $\sigma_{xy}$ is the cross covariance of $x$ and $y$, parameters $\alpha$, $\beta$ and $\gamma$ are used to adjust the relative importance of the three components, with $\alpha > 0$, $\beta > 0$ and $\gamma > 0$; $C_1, C_2, C_3$ are the constants to avoid instability when the denominators are very close to zero, $C_1 = (K_1 L)^2$, $C_2 = (K_2 L)^2$, $C_3 = C_2/2$, $K_1$, $K_2$ and $L$ are constants.

## 3 Data generation with Finite Element Method

### 3.1 Bridge models

Two adjacent steel-concrete composite bridges located in West Des Moines, Iowa, were simulated. Bridge 1 is 200 ft long and 38 ft wide with 3 spans, 5 longitudinal girders and 2 traffic lanes, while bridge 2 is 516 ft long and 29 ft wide with 5 spans, 4 longitudinal girders and 1 traffic lane. Planar-level finite element models of these two bridges were generated using 688 linear beam elements, 328 quadrilateral shell elements, 381 linear beam elements, and 162 quadrilateral shell elements in WinGen [35]. As shown in Fig. 1, the girders, stringers and floor beams were modeled using elastic beam elements, whereas the concrete deck was idealized using quadrilateral shell elements. The number of beam and shell elements of both bridges is shown in Table 1. Steel girder and stringer sections near piers were modeled as non-composite beams (yellow elements in Fig. 1), while those in the middle spans and side piers were modeled as composite ones (black elements in Fig. 1). Initial sections and material properties were assigned to all elements to match the design of two bridges. The boundary conditions were also idealized using rotational spring elements with appropriate initial stiffness [36]. A total of 25 and 36 strain gauges, for each bridge respectively, were attached to the bottom of the primary beam elements.

**TABLE 1**. Number of beam and shell elements for the bridge models.

| Item | | Bridge 1 | Bridge 2 |
|---|---|---|---|
| Beam elements | Girders | 200 | 216 |
| | Stringers | 160 | - |
| | Floor | 328 | 165 |
| Shell elements | | 320 | 162 |

Under damage conditions, the damage was assigned by reducing the moment of inertia of given girder elements, shown in Fig. 1. Damage levels of 5%, 10% and 20% were assigned by reducing the moment of inertia by 5%, 10% and 20%, respectively.

A total of 20 trucks were randomly selected from the truck library in WinGen and individually driven (in the simulations) on bridges. Strain data was collected and analyzed under normal condition and damaged conditions. As an example, strain data collected from sensor 10 (E 10) and sensor 28 (I 8) in bridge 2 under normal condition and different levels of damage is shown in Fig. 2 for Truck-101.

### 3.2 Headway simulation

In each simulations, trucks are driven over the bridged with a given time separating the lead truck and the following truck,

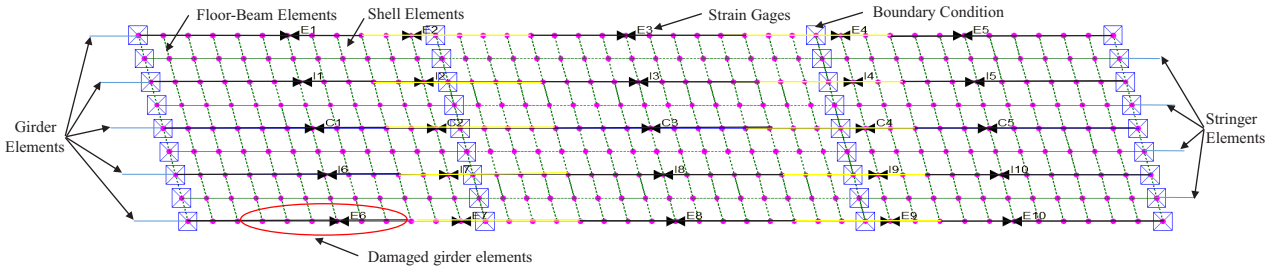


(a) Bridge 1

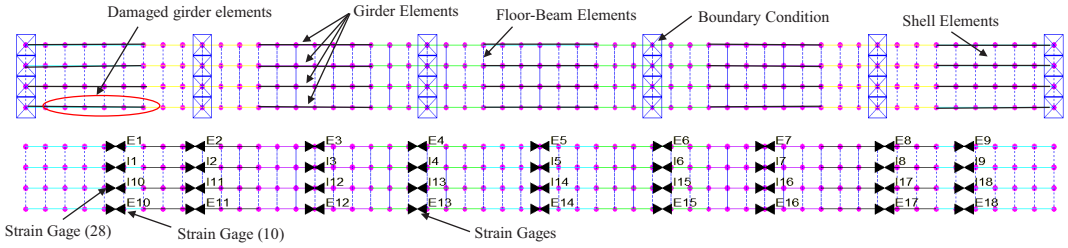


(b) Bridge 2

**FIGURE 1**. Modeling the bridges with Finite Element Method.

termed headway. Headway is generated from traffic modeling data found in [37]. Statistical parameters used to generate headway are listed in Table 2.

**TABLE 2**. Headway measured in reality [37], pair type: lead (truck) – follow (truck), SB – southbound, NB – northbound.

| Mean (sec) | | Median (sec) | | Std. dev. (sec) | |
|---|---|---|---|---|---|
| SB | NB | SB | NB | SB | NB |
| 2.92 | 2.86 | 2.71 | 2.71 | 1.43 | 1.46 |

A Random-walk Metropolis-Hastings sampler is applied to generate the headway set, and an example is shown in Fig. 3. With the simulated headway, strain data in each 20-truck set is generated, as shown in Fig. 4. When there is no truck on the bridge, the stain is taken as 0 (as only truck loading is considered in this work). When there is more than one truck on the bridge simultaneously, strain histories are added linearly. Bridge 2 contains more data set that include simultaneous trucks given its longer length relative to bridge 1.

### 3.3 Noise addition

In order to evaluate the robustness of the algorithm to noise in sensor data, noise is generated with a uniform distribution, and the amplitude is taken as 5% of the maximum of the measurements. The noisy strain data (regarding the strain data in Fig. 4) is shown in Fig. 5.

## 4 Damage detection framework for bridge network with spatiotemporal pattern network

### 4.1 Formation of STPN in truck matching between bridges

In this work, truck matching is referred as the successful identification of a truck driving sequence. Truck matching is critical to conduct the spatiotemporal study of structural behaviors on a network of bridges (Section 4.2), as they are taken as constant inputs. Although truck matching is beneficial in improving damage detection accuracy, it is not strictly required, as one may conduct spatiotemporal studies assuming that a given truck sequence remains constant between two adjacent bridges (no passing, no truck exiting/entering - more details provided in Section 4.2).

To implement truck matching, causality between sensors from the two bridges is applied to extract the features in the pairs. The basic idea is that the two sets of strain are unique in causality when the same truck passes on the bridges one after another. From the observations of the strain data from both bridges, the strain of the first bridge can be applied to predict the strain of the second bridge in spatiotemporal space, given that the same truck is passing on the bridges one after another.

To obtain the causal metric, the framework of STPN in truck matching is shown in Fig. 6. The procedure consists of five steps:

(1) Data abstraction.
(2) State transition formation via *D*-Markov machine.
(3) Extraction of causality in atomic patterns (APs) and relational patterns (RPs) with information based metric.
(4) Formation of similarity metric of each truck pair in the two bridges.

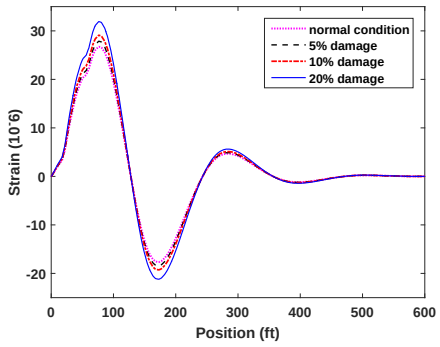


(a) Sensor 10 (damage span)

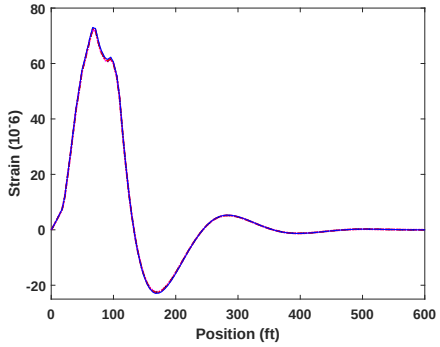


(b) Sensor 28

**FIGURE 2**. Bridge strain measured by sensors 10 and 28 (locations shown in Fig. 1) in bridge 2 under Truck-101. The damaged span (sensor 10) shows an increase in strain with increasing damage. The adjacent span (sensor 28) also exhibits a similar behavior, but at a much smaller scale.

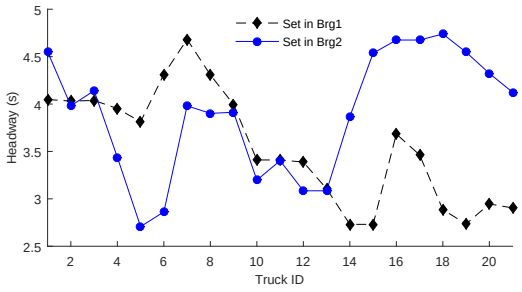


**FIGURE 3**. Example of generated headway.

(5) Truck matching via maximizing similarity between truck pairs.

The algorithm for truck matching is as follows.

**Algorithm 1.** Truck matching in bridges.

1 **Input**: Strain data $\{\mathbb{X}_i^n,\ i \in \mathbf{m}\}$ in bridge $n$ with truck set (IDs $\mathbf{m} = \{1, 2, \cdots,\ M\}$). Strain data $\tilde{X}_i^n$ with current truck (ID $i$) passing by.

2 **Output**: Matched truck set $\tilde{\mathbf{m}}$.

3 **Modeling and learning**.

4 Obtain symbol sequences $S$ with strain data $\mathbb{X}$ using the alphabet set $\Sigma$. Here, partitioning is implemented in two dimensional space, the strain from the sensor in bridge 1 is noted as the first dimension, and the strain from the sensor in bridge 2 is noted as the second dimension. The dimensions of $S$ are $g \times h$, representing number of sensors in bridge 1 and bridge 2 respectively.

5 Form the state sequences $\mathcal{Q}$ with symbol sequences $S$ using depth $D$ of PFSA.

6 **for all** $a \in \mathbf{g}$, $b \in \mathbf{h}$, **do**

7 Compute the state transition matrix $\Pi^{ab}$ with x$D$-Markov machine.

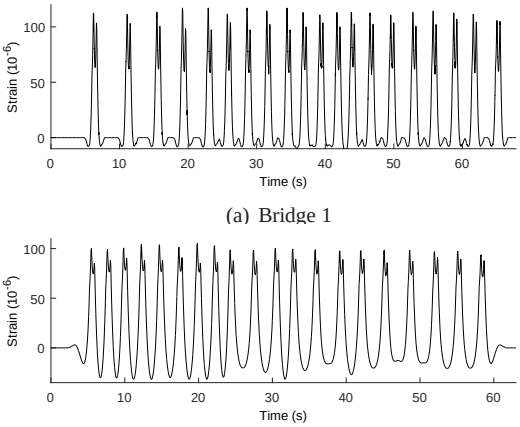


(a) Bridge 1

(b) Bridge 2

**FIGURE 4**. Simulated strain data at mid-span for both bridges with 20 trucks.

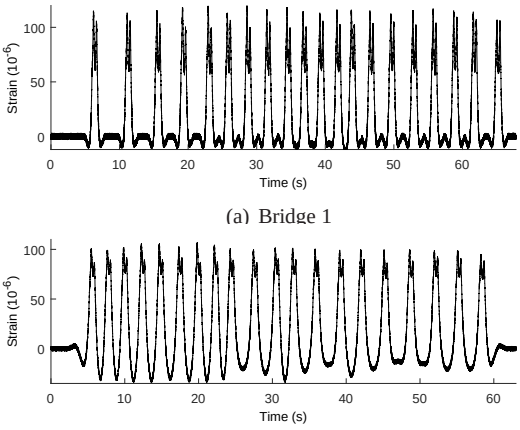


(a) Bridge 1

(b) Bridge 2

**FIGURE 5**. Strain of two bridges with noise. The same spans are shown as in Fig. 4.

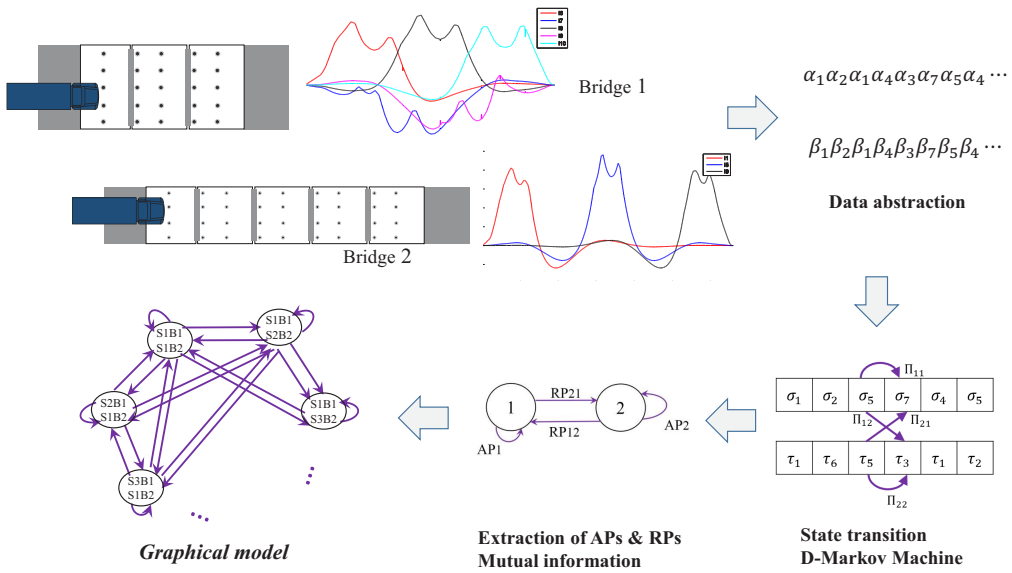


**FIGURE 6**. Framework in formation of spatiotemporal pattern network and graphical model for truck matching.

8 **end**
9 **for all** $a \in \mathbf{g}$, $b \in \mathbf{h}$, **do**
10 Compute the mutual information $\Lambda^{ab}$ with Eq. 1.
11 **end**
12 Repeat step 4-11, obtain the mutual information set $\{\Lambda_{g\times h}\}_{M\times M}$.
13 **Truck Matching**.
14 Obtain symbol sequences $\tilde{S}$ with strain data $\tilde{\mathbb{X}}$ using the alphabet set $\Sigma$.
15 Form the state sequences $\tilde{\mathscr{Q}}$ with symbol sequences $\tilde{S}$ using depth $D$ of PFSA.
16 Compute the state transition matrix $\tilde{\Pi}$ with x$D$-Markov machine.
17 Obtain the mutual information $\tilde{\Lambda}$ with Eq. 1.
18 **for all** $i \in \mathbf{m}$, $j \in \mathbf{m}$, **do**
19 Compute the similarity between $\tilde{\Lambda}$ and $\{\Lambda_{g\times h}\}_{ij}$, $i$ is the truck ID passing bridge 1, $j$ is the truck ID passing bridge 2.
20 **end**
21 Obtain the matching set $\tilde{\mathbf{m}}$ with maximal similarity.

## 4.2 Formation of STPN for damage detection

Bridges in the network are geographically close, the vehicle loads are therefore similar. Under this assumption, the causality between the bridges is relatively stable and consistent. If damage is induced in one bridge in some aspect, e.g., span damage due to external effect, the causality between the damaged bridge and other bridges would change.

To detect the damage of the bridge in the above situation, this work applies STPN in estimating the variation of causality between the bridges. The steps in data abstraction, state transition formation, and extraction of casuality are similar to Section 4.1, the damage detection approach is shown in Fig. 7. Two STPNs are formed in the normal condition and anomaly (damage) condition, respectively, and the variation of the causality is compared pattern by pattern. The expectation is that the damaged location will present increased strain and this can be captured by causality metric in STPN. The damage detection approach also provides a view for damage localization as the sensor presenting variation of causality indicates the damage position where the sensor installs.

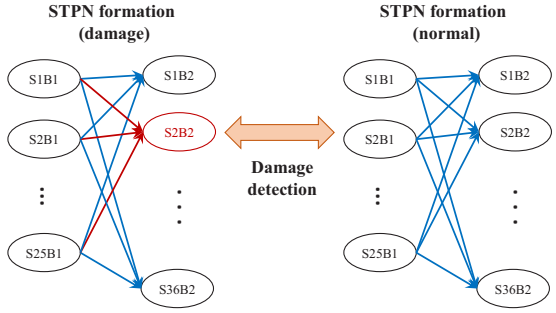


**FIGURE 7**. Formation of STPNs for damage detection in two bridges.

The algorithm for damage detection is as follows.

**Algorithm 2.** Damage detection for in bridges with similar truck set passing by.

1 **Input**: Strain data $\{\mathbb{X}_i^n,\ i \in \mathbf{m}\}$ in bridge $n$ with truck set (IDs $\mathbf{m} = \{1,2,\cdots,M\}$). Strain data with damage $\{\tilde{\mathbb{X}}_i^n\}$ in bridge $n$ with truck (IDs $\mathbf{m} = \{1,2,\cdots,M\}$).

**Output**: Damage level and location.
**Modeling in normal condition**.
Obtain symbol sequences $S$ with strain data $\mathbb{X}$ using the alphabet set $\Sigma$. Here, symbolization is implemented in one dimensional space regarding time series generated from a single sensor. The numbers of sensors in bridge 1 and bridge 2 are $U$ and $V$, respectively.
Form the state sequences $\mathscr{Q}$ with symbol sequences $S$ using depth $D$ of PFSA.
**for all** $a \in \mathbf{U}$, $b \in \mathbf{V}$, **do**
    Compute the state transition matrix $\Pi^{ab}$ with x$D$-Markov machine.
**end**
**for all** $a \in \mathbf{U}$, $b \in \mathbf{V}$, **do**
    Compute the mutual information $\Lambda^{ab}$ with Eq. 1.
**end**
**Modeling in anomalous condition**.
Obtain symbol sequences $\tilde{S}$ with strain data $\tilde{\mathbb{X}}$ using the alphabet set $\Sigma$. Here, symbolization is implemented in one dimensional space regarding time series generated from a single sensor. The numbers of sensors in bridge 1 and bridge 2 are $U$ and $V$, respectively.
Form the state sequences $\tilde{\mathscr{Q}}$ with symbol sequences $\tilde{S}$ using depth $D$ of PFSA.
**for all** $a \in \mathbf{U}$, $b \in \mathbf{V}$, **do**
    Compute the state transition matrix $\tilde{\Pi}^{ab}$ with x$D$-Markov machine.
**end**
**for all** $a \in \mathbf{U}$, $b \in \mathbf{V}$, **do**
    Compute the mutual information $\tilde{\Lambda}^{ab}$ with Eq. 1.
**end**
**Inference**.
Compute the difference between $\{\tilde{\Lambda}\}$ and $\{\Lambda\}$, to obtain the damage level and location.

It should be noted that the algorithms for truck matching and damage detection are based on two bridges in this work. However, the approach can be easily extended to the bridge network with multiple bridges, where the relations in the bridge network can be considered pairwise. STPNs formed in truck matching and damage detection are different in structure, further work will pursue a unified framework in processing feature extraction for both truck matching and damage detection.

## 5 Results and discussions

### 5.1 Truck matching

Truck matching is carried out in two cases: (1) the order of the two truck sets are identical, with the assumption that there is no passing of trucks between the bridges, and (2) the orders are different, and the passing of trucks is random. The truck matching results are shown in Fig. 8. The IDs in defined orders and matched orders are listed in Table. 3.

In the two cases, the trucks 4 and 5 are mismatched. The reason is that the weights and dimensions of the two trucks are similar, and the strain caused by the two trucks are very close (as shown in Fig. 9).

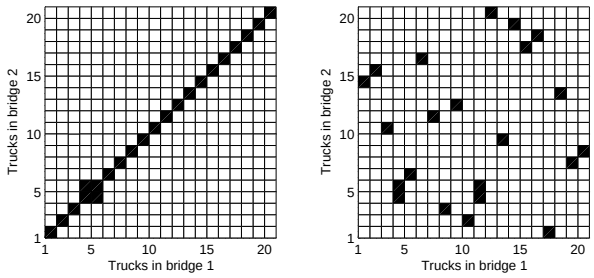


(a) Case 1, trucks in same order (b) Case 2, trucks in different order

**FIGURE 8**. Truck matching results. The block in black shows the matching result and the detected truck IDs are in x-axis and y-axis respectively.

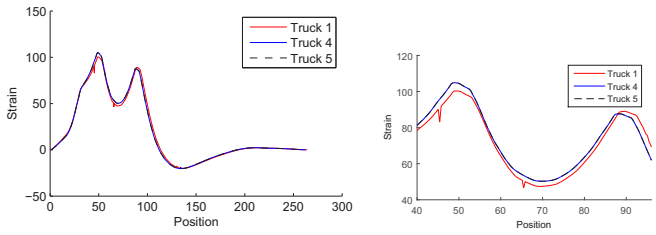


(a) Local strain of bridge 1

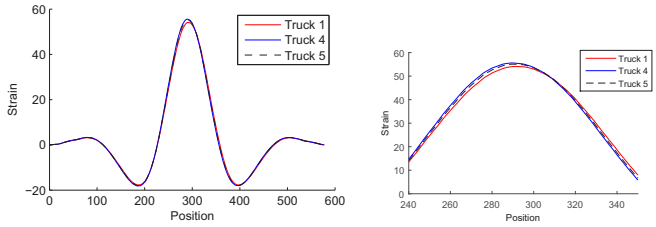


(b) Local strain of bridge 2

**FIGURE 9**. Strain in mismatched trucks (trucks 4 & 5, unit in $10^{-6}$).

The case presented above includes noiseless data. The accuracy in truck matching may be decreased with diverse noise levels. Further work is being conduction on the truck matching algorithm for noisy data sets.

### 5.2 Damage detection

Damage detection is implemented with the same truck sets used in the above section, where the damage data in bridge 2 is applied. With the normal and damage data in the bridge 2, the patterns of the STPNs are computed and the variation between

**TABLE 3**. Truck matching results in two cases.

| Item | | | Truck Set (IDs) |
|---|---|---|---|
| Case 1 | Defined | Bridge 1 | 1-20 |
| | | Bridge 2 | 1-20 |
| | Matched | Bridge 2 | 1-20 (4,5 mismatched) |
| Case 2 | Defined | Bridge 1 | 1-20 |
| | | Bridge 2 | 14, 15, 10, 5, 6, 16, 11, 3, 12, 2, 4, 20, 9, 19, 17, 18, 1, 13, 7, 8 |
| | Matched | Bridge 2 | 14, 15 10, 4/5, 6, 16, 11, 3, 12, 2, 4/5, 20, 9, 19, 17, 18, 1, 13, 7, 8 |

them is used for damage detection. Here, the same truck set is used to generate the stain data in bridge 1 and bridge 2 (normal and damage cases respectively). The damage detection results are shown in Figs. 10 and 11 in terms of the data without noise and with noise, respectively.

The damage level can be seen from the detection results. Furthermore, the results indicate the damage span. The abnormal patterns exist between sensor 10 of bridge 2 and any sensor in bridge 1 in Fig. 10. This means that the damage is located in the span with sensor 10. A similar case is observed in Fig. 11, where most of the abnormal patterns locate between sensor 10 of bridge 2 and most of the sensors in bridge 1. Some of the patterns (e.g., (1, 10) and (2, 10)) do not show anomaly, the reason is that the signal with small amplitude is smaller than the amplitude of the noise. Also, some anomalous patterns (e.g. (23, 6) and (23, 15)) are induced by the noise.

Note, sensor 28 of bridge 2 in Figs. 10 and 11 shows slight anomaly, and this is because the sensor is adjacent to the damaged span, as shown in Fig. 2, where weak increases of strain in sensor 28 can be observed.

### 5.3 Discussions

This work applied simulation data in truck matching and damage detection in bridge network, and the simulation data is generated by finite element method based on two existing bridges. The noise is added with a predefined amplitude and uniform distribution. Further analysis is being carried out to analyze typical characteristics of strain gauges used in bridge monitoring to get more field-like signals. Also, the trucks used in this work are randomly picked; further work is being implemented in generating more data sets to cover typical dimensions and weights of diverse trucks.

Regarding understanding the causal relations between bridges in terms of truck matching and damage detection, this work applied spatiotemporal pattern network with the simulation data in two bridges. The results show that the proposed approach can effectively discover the behavior of the strain responses with different trucks passing bridges, and detect the abnormal damage in a bridge by estimating the variation of causal relationship between two bridges geographically close. With the ability in processing large-scale dataset, the proposed approach can be applied in complex network with dense sensor networks, and the application provides a novel view in damage detection via exploring causality between bridge network.

## 6 Conclusions

With spatiotemporal pattern network, this work conducted truck matching and damage detection for a small bridge network composed of two adjacent bridges. The proposed approach is designed for processing large-scale dataset in a bridge network (network of dense sensor network), and the results show the advantages of the proposed approach in: (i) capturing spatiotemporal features to discover causality between bridges (geographically close), (ii) handling noise in data for feature extraction, and (iii) detecting and localizing damage via comparing the behaviors in the bridge network.

The proposed approach for the damage detection is based on the data generated by multiple trucks. The current application is implemented in two bridges with one-span damage case. The further work will pursue: (i) integrating truck matching and damage detection in a unified framework to implement online damage detection, (ii) damage detection in multiple cases with diverse damage levels, (iii) detecting damage with typical noise level regarding the sensor type and environment conditions.

## ACKNOWLEDGMENT

This paper is based upon research partially supported by the National Science Foundation under Grant No. CNS-1464279 and Grant No. CMMI-1463252. Any opinions, findings, and conclusions or recommendations expressed in this material are those of the authors and do not necessarily reflect the views of the National Science Foundation.

## REFERENCES

[1] Brownjohn, J., 2007. “Structural health monitoring of civil infrastructure”. *Philosophical Transactions of the Royal*

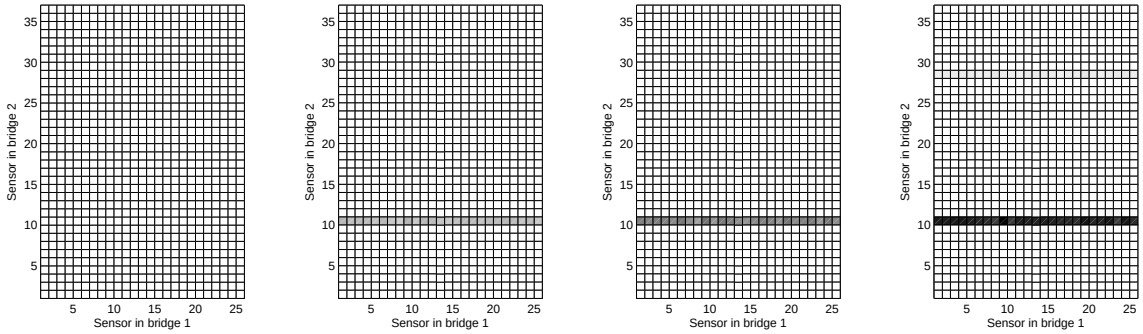


(a) Normal (b) Damage, 5% (c) Damage, 10% (d) Damage, 20%

**FIGURE 10**. Damage detection results. The gray map represents the anomaly degree of the pattern between the sensors (IDs in x-axis and y-axis respectively)

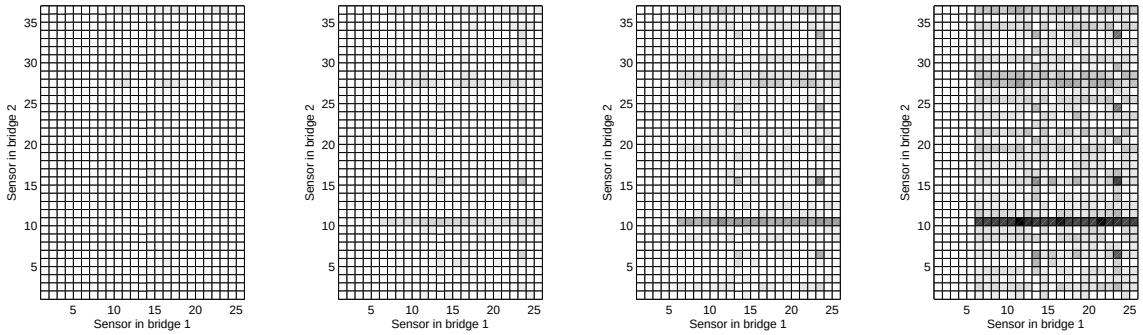


(a) Normal (b) Damage, 5% (c) Damage, 10% (d) Damage, 20%

**FIGURE 11**. Damage detection results (with noise). The gray map represents the anomaly degree of the pattern between the sensors (IDs in x-axis and y-axis respectively)

*Society A: Mathematical, Physical and Engineering Sciences*, ***365***(1851), pp. 589–622.

[2] Harms, T., Sedigh, S., and Bastianini, F., 2010. "Structural health monitoring of bridges using wireless sensor networks". *Instrumentation & Measurement Magazine, IEEE*, ***13***(6), pp. 14–18.

[3] Simon, J., Bracci, J., and Gardoni, P., 2010. "Seismic response and fragility of deteriorated reinforced concrete bridges". *Journal of Structural Engineering*, ***136***(10), pp. 1273–1281.

[4] Kharroub, S., Laflamme, S., Song, C., Qiao, D., Phares, B., and Li, J., 2015. "Smart sensing skin for detection and localization of fatigue cracks". *Smart Materials and Structures*, ***24***(6), p. 065004.

[5] Yu, L., Giurgiutiu, V., Ziehl, P., Ozevin, D., and Pollock, P., 2010. "Steel bridge fatigue crack detection with piezoelectric wafer active sensors". In SPIE Smart Structures and Materials+ Nondestructive Evaluation and Health Monitoring, International Society for Optics and Photonics, pp. 76471Y–76471Y.

[6] Gresil, M., Yu, L., Shen, Y., and Giurgiutiu, V., 2013. "Predictive model of fatigue crack detection in thick bridge steel structures with piezoelectric wafer active sensors". *Smart Structures and Systems*, ***12***(2), pp. 1738–1584.

[7] Tsuda, H., Lee, J.-R., Guan, Y., and Takatsubo, J., 2007. "Investigation of fatigue crack in stainless steel using a mobile fiber bragg grating ultrasonic sensor". *Optical Fiber Technology*, ***13***(3), pp. 209–214.

[8] Lee, D., Lee, J., Kwon, I., and Seo, D., 2001. "Monitoring of fatigue damage of composite structures by using embedded intensity-based optical fiber sensors". *Smart Materials and Structures*, ***10***(2), p. 285.

[9] DAlessandro, A., Ubertini, F., Materazzi, A. L., Laflamme, S., and Porfiri, M., 2014. "Electromechanical modelling of a new class of nanocomposite cement-based sensors for structural health monitoring". *Structural Health Monitoring*, p. 1475921714560071.

[10] Ubertini, F., Materazzi, A. L., D'Alessandro, A., and Laflamme, S., 2014. "Natural frequencies identification of a reinforced concrete beam using carbon nanotube cement-based sensors". *Engineering Structures*, ***60***, pp. 265–275.

[11] Tung, S., Yao, Y., and Glisic, B., 2014. "Sensing sheet: the sensitivity of thin-film full-bridge strain sensors for crack detection and characterization". *Measurement Science and Technology*, ***25***(7), p. 075602.

[12] Wu, J., Song, C., Saleem, H. S., Downey, A., and

Laflamme, S., 2015. "Network of flexible capacitive strain gauges for the reconstruction of surface strain". *Measurement Science and Technology,* ***26***(5), p. 055103.

[13] Bocchini, P., and Frangopol, D. M., 2011. "Connectivity-based optimal scheduling for maintenance of bridge networks". *Journal of Engineering Mechanics,* ***139***(6), pp. 760–769.

[14] Coalition, S. T., 2013. "Demonstration of load rating capabilities through physical load testing".

[15] Saydam, D., Bocchini, P., and Frangopol, D. M., 2013. "Time-dependent risk associated with deterioration of highway bridge networks". *Engineering Structures,* ***54***, pp. 221–233.

[16] Fitzsimmons, E. J., Mulinazzi, T. E., and Schrock, S. D., 2014. "Economic impact of closing structurally deficient or functionaly obsolete bridges on very low-volume roads". In Transportation Research Board 93rd Annual Meeting, pp. 14–4486.

[17] Moniz, L., Nichols, J., Nichols, C., Seaver, M., Trickey, S., Todd, M., Pecora, L., and Virgin, L., 2005. "A multivariate, attractor-based approach to structural health monitoring". *Journal of Sound and Vibration,* ***283***(1-2), pp. 295–310.

[18] Overbey, L., Olson, C., and Todd, M., 2007. "A parametric investigation of state-space-based prediction error methods with stochastic excitation for structural health monitoring". *Smart Materials and Structures,* ***16***, pp. 1621–1638.

[19] Monroig, E., 2009. "Detection of Changes in Dynamical Systems by Nonlinear Time Series Analysis". PhD thesis, University of Tokyo.

[20] Figueiredo, E., Todd, M., Farrar, C., and Flynn, E., 2010. "Autoregressive modeling with state-space embedding vectors for damage detection under operational variability". *International Journal of Engineering Science,* ***48***(10), pp. 822–834.

[21] Liu, G., Mao, Z., Todd, M. D., and Huang, Z., 2013. "Damage assessment with state-space embedding strategy and singular value decomposition under stochastic excitation". *Structural Health Monitoring*, pp. 131–142.

[22] Rabin, N., and Averbuch, A., 2010. "Detection of anomaly trends in dynamically evolving systems.". In AAAI Fall Symposium: Manifold Learning and Its Applications.

[23] Huang, Y., Zha, X. F., Lee, J., and Liu, C., 2013. "Discriminant diffusion maps analysis: A robust manifold learner for dimensionality reduction and its applications in machine condition monitoring and fault diagnosis". *Mechanical Systems and Signal Processing,* ***34***(1), pp. 277–297.

[24] Rao, C., Ray, A., Sarkar, S., and Yasar, M., 2009. "Review and comparative evaluation of symbolic dynamic filtering for detection of anomaly patterns". *Signal, Image and Video Processing,* ***3***(2), pp. 101–114.

[25] Sarkar, S., Sarkar, S., Virani, N., Ray, A., and Yasar, M., 2014. "Sensor fusion for fault detection and classification in distributed physical processes". *Frontiers in Robotics and AI,* ***1***, p. 16.

[26] Jiang, Z., and Sarkar, S., 2015. "Understanding wind turbine turbine interactions using spatiotemporal pattern network". In Proceedings of ASME Dynamics Systems and Control Conference.

[27] Liu, C., Ghosal, S., Jiang, Z., and Sarkar, S., 2016. "An unsupervised spatiotemporal graphical modeling approach to anomaly detection in distributed cps". In Proceedings of the International Conference of Cyber-Physical Systems, (Vienna, Austria).

[28] Sarkar, S., Srivastav, A., and Shashanka, M., 2013. "Maximally bijective discretization for data-driven modeling of complex systems". In American Control Conference (ACC), 2013, IEEE, pp. 2674–2679.

[29] Sarkar, S., and Srivastav, A., 2016. "A composite discretization scheme for symbolic identification of complex systems". *Signal Processing,* ***125***, pp. 156 – 170.

[30] Wibral, M., Rahm, B., Rieder, M., Lindner, M., Vicente, R., and Kaiser, J., 2011. "Transfer entropy in magnetoencephalographic data: Quantifying information flow in cortical and cerebellar networks". *Progress in biophysics and molecular biology,* ***105***(1), pp. 80–97.

[31] Solo, V., 2008. "On causality and mutual information". In Decision and Control, 2008. CDC 2008. 47th IEEE Conference on, IEEE, pp. 4939–4944.

[32] Papadimitriou, P., Dasdan, A., and Garcia-Molina, H., 2010. "Web graph similarity for anomaly detection". *Journal of Internet Services and Applications,* ***1***(1), pp. 19–30.

[33] Wang, Z., Bovik, A. C., Sheikh, H. R., and Simoncelli, E. P., 2004. "Image quality assessment: from error visibility to structural similarity". *Image Processing, IEEE Transactions on,* ***13***(4), pp. 600–612.

[34] Liu, C., Jiang, D., and Yang, W., 2014. "Global geometric similarity scheme for feature selection in fault diagnosis". *Expert Systems with Applications,* ***41***(8), pp. 3585–3595.

[35] Bridge Diagnostics Inc., 2001. User's manual: WinGen.

[36] Seo, J., Phares, B., Lu, P., Wipf, T., and Dahlberg, J., 2013. "Bridge rating protocol using ambient trucks through structural health monitoring system". *Engineering Structures,* ***46***, pp. 569–580.

[37] Houchin, A., Dong, J., Hawkins, N., and Knickerbocker, S., 2015. "Measurement and analysis of heterogenous vehicle following behavior on urban freeways: Time headways and standstill distances". In Intelligent Transportation Systems (ITSC), 2015 IEEE 18th International Conference on, IEEE, pp. 888–893.